Block Copolymers under Cylindrical Confinement

Hongqi Xiang, Kyusoon Shin, Taehyung Kim, Sung In Moon, Thomas J. McCarthy,* and Thomas P. Russell*

Polymer Science and Engineering Department, University of Massachusetts, Amherst, Massachusetts 01003

Received April 9, 2004; Revised Manuscript Received May 7, 2004

ABSTRACT: Microphase-separated block copolymers were introduced as melts into nanoscopic cylindrical pores in alumina membranes via capillary action. The geometric confinement of both lamellar and cylindrical microdomain morphologies of styrene/butadiene block copolymers, PS-*b*-PBD, was investigated by transmission electron microscopy. Well-developed microphase-separated structures were formed within the resulting nanorods. Polymers that exhibit cylindrical microdomains in the bulk orient with cylindrical microdomains along the nanorod axis due to the preferential segregation of the PBD block to the walls of the pores. The period and packing of the microdomains differ from those observed in the bulk due to an incommensurability between the pore geometry and the natural period and hexagonal packing of the copolymer microdomains. With polymers exhibiting bulk lamellar morphology, confinement forces the formation of concentric cylinders oriented along the nanorod axis. The number of concentric cylinders depends on the ratio of the nanorod diameter to the equilibrium period of the copolymer. Because of the preferential segregation of PBD at the alumina surface, either PBD or PS can form the central core. These results indicate a method by which copolymer microdomains can be manipulated in a simple manner for the fabrication of isolated nanostructures.

Introduction

Phase separation in confined systems has been the subject of extensive theoretical and experimental studies (see ref 1, for example). The fundamental scientific interest stems from the influence of commensurability on structure and phase transitions of confined systems. The intriguing prospects from a technological viewpoint are the novel morphologies that can be achieved and can serve as scaffolds for nanostructures. An interesting class of materials for such studies is block copolymers, due to their rich phase behavior and ordering transitions, that can be studied under relatively simple experimental conditions.[2]

Symmetric diblock copolymers are comprised of two chemically distinct polymer chains covalently bonded together at one end with volume fractions of each constituent equal to 0.5. In the bulk, these copolymers microphase separate into lamellar microdomains with a characteristic equilibrium period L_0, where grains of ordered lamellar microdomains are randomly oriented.[2] In thin films, the interactions between the blocks and the air and substrate interfaces can cause preferential segregation of one of the blocks to the interfaces, forcing an orientation of the microdomains parallel to the interfaces, resulting in a multilayered structure.[3−14] If one block segregates to both interfaces (symmetric wetting), the film thickness is controlled by nL_0, where n is an integer. In the case of asymmetric wetting, the film thickness is $(n + {}^1/_2)L_0$. Incommensurability occurs when n is nonintegral. For thin films on a solid substrate with a free surface, incommensurability is circumvented by the formation of islands or holes at the free surface with step height L_0. If the film is confined between two rigid solid interfaces, the formation of surface topography is not possible. For lamellar microdomains oriented parallel to the confining interfaces, the period of the confined multilayers can change in response to this frustration. If interfacial interactions are balanced, the lamellar microdomains orient normal to the interfaces, eliminating an elastic deformation of the chains. Asymmetric diblock copolymers, on the other hand, have drawn much less attention.[15−18] As in the case of symmetric diblock copolymers, the interplay of the confinement with the preferential interfacial interactions causes deviations of the morphology from that seen in the bulk.

Most studies to date have focused on block copolymers confined between parallel solid walls, effectively a one-dimensional confinement. Much less attention has been paid to two- or three-dimensional confinement, though multidimensional confinement is common in nature. Quite recently, He et al.[19] and Fraaije et al.[20] performed simulations on symmetric block copolymers confined in cylindrical pores, a two-dimensional confinement. Depending on the strength of the interactions between the copolymer and the pore walls, two equilibrium morphologies were predicted. In the case of weak interactions, the lamellae were predicted to orient normal to the cylinder axis as a stacked-disk morphology. With strong interactions, concentric cylinders were predicted over a wide range of pore radii and polymer chain length.[20]

In the study presented here, both symmetric and asymmetric diblock copolymers were investigated under two-dimensional confinement using nanoporous anodized aluminum membranes. The block copolymers were introduced as melts into the cylindrical pores of the membrane, and the membrane was removed, forming free-standing nanorods of the microphase-separated copolymer. We recently reported this procedure for the preparation of homopolymer nanorods.[21] Perturbations of the bulk morphology were observed for the copolymers, giving rise to novel nanoscopic structures.

* To whom correspondence should be addressed. Russell: Tel 413-577-1535; Fax 413-577-1510; e-mail russell@mail.pse.umass.edu. McCarthy: Tel 413-577-1512; Fax +1-413-577-1510; e-mail tmccarthy@polysci.umass.edu.

10.1021/ma049299m CCC: $27.50
Published on Web 06/25/2004

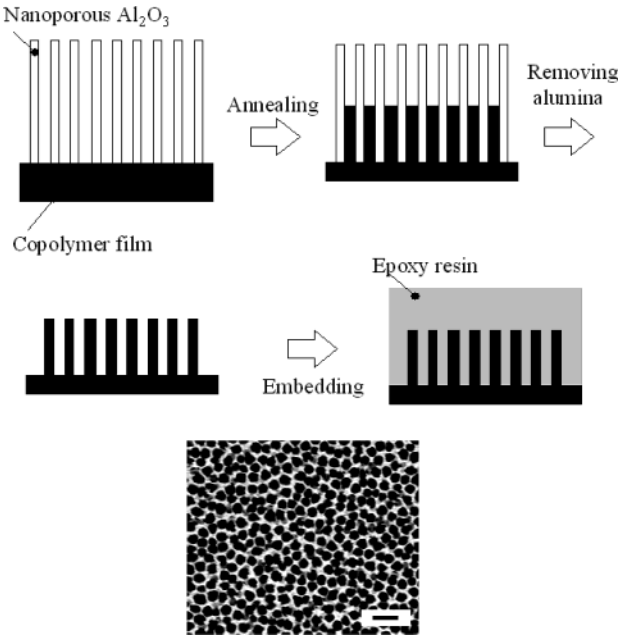

Figure 1. Schematic for confining block copolymers in nanoporous alumina template. The SEM image is the top view of nanoporous anodized aluminum membranes, Whatman Anodics 200 nm. Scale bar: 1 μm.

Experimental Section

Anodized aluminum membranes, Anodisc 0.2 μm, were purchased from Whatman, Inc. These membranes are free-standing disks with a diameter of 13 mm and a thickness of 60 μm. Figure 1 shows a SEM image of a nanoporous membrane. The membranes are comprised of straight, cylindrical pores, oriented normal to the disk surface. The pores range in diameter from ~100 to ~350 nm. As can be seen, some pores impinge upon one another, forming larger, non-circular pores. Symmetric and asymmetric diblock copolymers of styrene and butadiene (PS-*b*-PBD) were purchased from Polymer Sources. The asymmetric PS-*b*-PBD had a number-average molecular weight, M_n, of 42 000 and a polydispersity, M_w/M_n, of 1.03 with a volume fraction of ~0.36 PBD. The bulk morphology consists of PBD cylinders in a PS matrix with a cylinder-to-cylinder distance of ~29.1 nm, as measured by small-angle X-ray scattering (SAXS). The symmetric PS-*b*-PBD had a M_n of 42 000 with M_w/M_n of 1.03 with a volume fraction of ~0.56 PBD. The bulk morphology was lamellar with an equilibrium period of ~29.6 nm (SAXS).

Figure 1 shows a schematic diagram of the process used to introduce the copolymer into the cylindrical alumina pores. Films (~15 μm in thickness) of the copolymers were solvent cast from toluene solutions onto glass slides and dried. The aluminum oxide membrane was then placed on top of the copolymer film. The assembly was heated to 125 °C, which is above the glass transition temperatures of both blocks. The copolymer melt entered into the pores of the membrane via capillary action. After annealing for 24 h under vacuum, the copolymer/membrane assembly was quenched to room temperature. The alumina membrane was removed using 5 wt % sodium hydroxide (water/methanol 8:2 v/v),[21] leaving an array of copolymer nanorods protruding from the copolymer film like the bristles of a brush. The morphology of the copolymer nanorods was investigated using a JEOL 6320 model scanning electron microscope at an accelerating voltage of 5 kV.

Bright field transmission electron microscopy (TEM) studies were conducted with a JEOL 100CX TEM operating at an accelerating voltage of 100 kV. To prepare TEM specimens, the copolymer film with protruding nanorods was stained with OsO_4, embedded in an epoxy resin, and cured at 60 °C for 24 h. Ultrathin sections were prepared using a Leica Ultracut microtome equipped with a diamond knife.

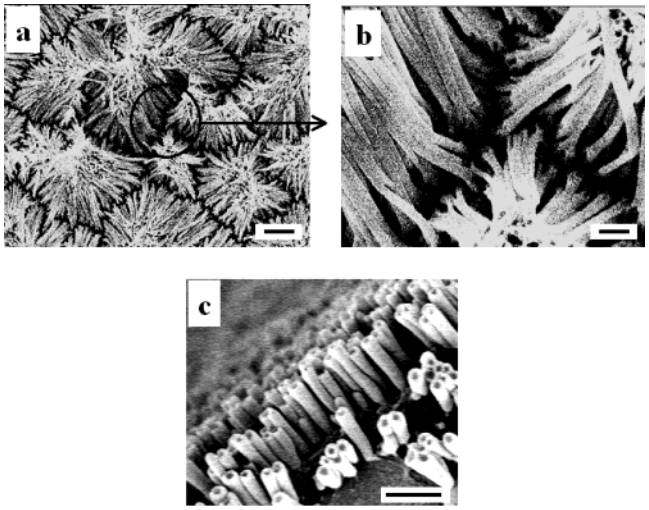

Figure 2. SEM micrographs of PS-*b*-PBD nanorods after removing alumina template. Scale bars: 2.5 μm (a), 500 nm (b), and 1 μm (c).

Results and Discussion

Figure 2 shows SEM micrographs of the asymmetric copolymer nanorods after complete removal of the template. The surfaces of the nanorods are smooth and of uniform length. The nanorods have a high aspect ratio, ~15:1 and, after being freed from the nanoporous template, do not stand erect on the supporting copolymer film but collapse onto each other. When shorter rods (~5:1 aspect ratio) are prepared (by reducing the time of membrane−polymer contact), individual copolymer nanorods do not collapse (Figure 2c). The surface layer of the copolymer nanorods consists of PBD (as discussed later). PBD has a glass transition temperature of ~−95 °C; thus, the surfaces of the nanorods are tacky at room temperature, and this is the likely cause of nanorod clustering. This was not observed with homopolystyrene nanorods.[21] At higher magnification, the top surfaces of the rods are dark, suggesting a depression in the center of the nanorod ends. This depressed center is consistent with a meniscus at the end of the nanorod, indicating that the copolymer wets the pore walls.

Generation of the nanorods involves capillary force that drives the copolymer melt into the cylindrical nanopores. The capillary force originates from a reduction in free energy that occurs by replacing the air/wall interface with a copolymer/wall interface. If the capillary force is positive, i.e., if the contact angle between the copolymer melt and the capillary wall is less than 90°, the copolymer spontaneously enters the capillary.[22] The maximum height that the copolymer melt can rise within the capillary can, to a first approximation, be obtained by[23]

$$h_{max} = (2\gamma_{copolymer/air} \cos \theta)/(\rho g r) \qquad (1)$$

where h_{max} is the maximum height, $\gamma_{copolymer/air}$ the surface tension of the copolymer melt, θ the contact angle at the copolymer/capillary wall interface, ρ the density of the copolymer, g the gravitational constant, and r the pore radius. The contact angle, estimated from the meniscus seen in the cross-sectional TEM image (discussed later), is ~80°. The surface tension of polybutadiene is ~30 mN/m. Using a PS-*b*-PBD density of 0.95 g/cm^3 and pore diameter 200 nm, a maximum height of 11.2 m is predicted from eq 1. This result

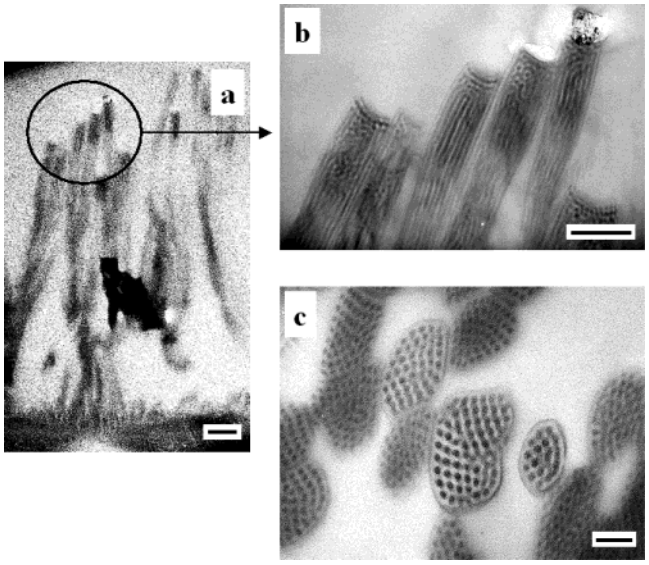

Figure 3. TEM cross-sectional images of cylindrical PS-*b*-PBD confined in cylindrical pores. (a, b) Views along pore. Scale bars: 500 nm. (c) View across pore. Scale bar: 100 nm.

indicates that the length and aspect ratio of the copolymer nanorods may be made quite large.

The time required to fill the nanopores with the copolymer can be estimated by[22,23]

$$t = 2\eta z^2/(R\gamma_{\text{copolymer/air}} \cos\theta) \qquad (2)$$

where t is the time, η the viscosity of the copolymer melt, z the length of the capillary, and R the hydraulic radius (the cross-sectional area of a stream divided by the wetted perimeter, here $R = 0.5r$). The viscosity of PS-*b*-PBD is about 10^6 Pa s.[23] According to eq 2, t is ~26 h for the copolymer melt to fill the cylindrical pores to a height of ~5 μm. It should be noted that in the above calculation the microphase separation of the block copolymer melt was not considered and that the PS-*b*-PBD is in the strong segregation limit. The microphase separation should retard or even stop the flow of the copolymer melt into the nanopores. Taking these points into consideration, the calculated time is in remarkably good agreement with the actual time of 24 h used experimentally.

To visualize the microphase-separated morphology in the copolymer nanorods, TEM studies were performed. Figure 3a shows a cross-sectional TEM image along the nanorod axis of asymmetric PS-*b*-PBD. The copolymer at the base of the pores was not removed, so both copolymer that was outside of and within the pores can be observed in Figure 3a. This image shows that the copolymer melt flowed from the film into the pores, forming copolymer nanorods with a high aspect ratio. A typical hexagonally packed array of cylindrical microdomains was seen for the PS-*b*-PBD copolymer outside of the pores. At the end of the copolymer nanorods, a meniscus is clearly seen in the cross-sectional view at higher magnification (Figure 3b). This is the signature of the capillary rise. Within the nanorods, the microphase-separated morphology of the copolymer is well developed. The PBD phase was preferentially stained with OsO_4 and appears darker than the PS matrix. It can be seen that the PBD preferentially segregates to both the interface with the nanopore wall and the free surface, highlighting the edges of the columns. Within the columns, the PBD cylinders appear as dark lines

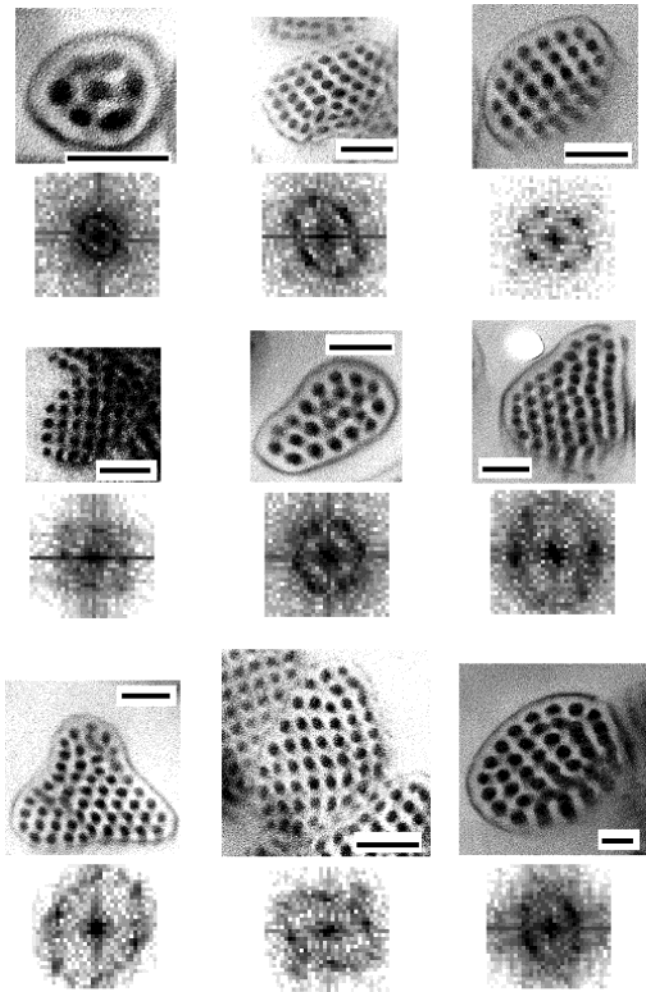

Figure 4. TEM cross-sectional images of cylindrical PS-*b*-PBD in pores of different geometry along with the corresponding FFT's. Scale bars: 100 nm.

parallel to the axes of the nanorods. At the top of the nanorods, at the air/copolymer interface, a change in the orientation of the cylindrical domains is observed, evidenced by the dark dots for the PBD cylinders. Figure 3c shows a cross-sectional TEM image for the asymmetric PS-*b*-PBD nanorods cut normal to the nanorod axis. A rim of PBD is seen around the edges of the sections, which is consistent with the sections cut along the nanorod axis. It should be noted that microtoming the section absolutely normal to the column axis is experimentally difficult. Thus, most of the cross sections are elliptical rather than circular. Even still, information relevant to the microphase-separated morphology can be obtained. In the ellipses, circularly shaped PBD domains are observed, indicating an orientation of PBD cylinders along the pore axes.

Figure 1 indicates that the shape and size of the nanopores of the commercial alumina template are not uniform. Consequently, the structure of the copolymer nanorods also varies in different pores. This variation provides a means to probe one sample under different confinement conditions. Figure 4 shows some of the morphologies observed for the asymmetric PS-*b*-PBD confined within nanopores having different geometries. For each image, a fast Fourier transform (FFT) was obtained to analyze the packing of the cylindrical microdomains. The FFT shows immediately that the hexagonal packing of the cylindrical domains is main-

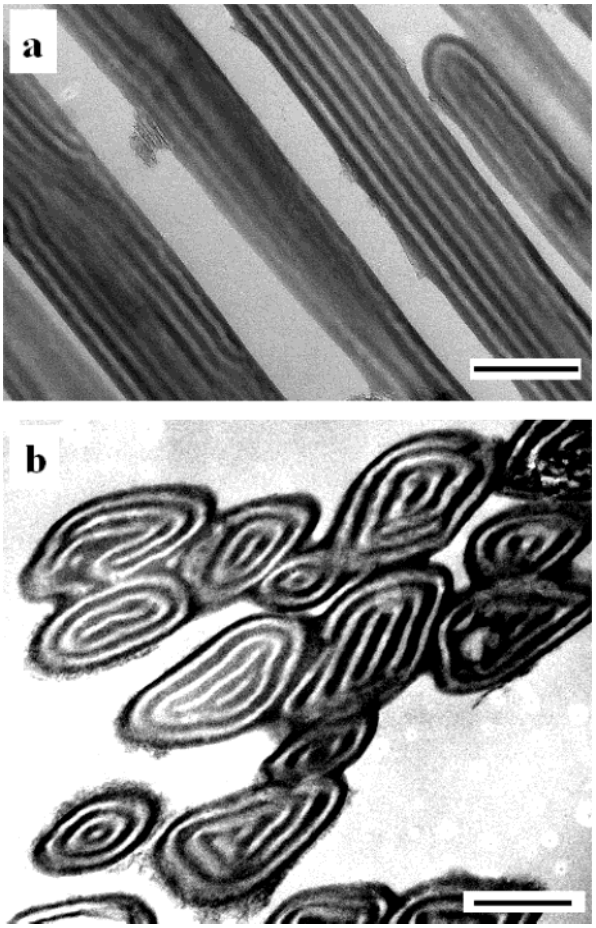

Figure 5. TEM cross-sectional images of lamellar PS-*b*-PBD confined in cylindrical pores. (a) View along pore. (b) View across pore. Scale bars: 200 nm.

tained, but the shapes and sizes of the pores can place severe constraints on the packing. In nearly all cases, six spots are seen indicative of the hexagonal packing. However, both the symmetry and separation distance of the domains can be altered. For nearly circular pores, though, only one grain is found for the cylindrical microdomains. As the pore diameter decreases, fewer cylinders are confined in the pores and for a pore diameter ~120 nm, only seven cylinders are formed within the pore. It should also be noted that the circular shape of cylindrical confinement does not match the geometrical requirement for hexagonal packing of the cylindrical microdomains. The constraint can be distributed over fewer layers in the case of a copolymer confined in small pores, and a large change in the apparent period and morphology must occur. This is being investigated further using well-defined membranes with pore diameters less than 100 nm.

Figure 5a shows a TEM cross-sectional image, microtomed along the column axis, for nanorods prepared using symmetric PS-*b*-PBD. Alternating dark (PBD) and bright (PS) lines parallel to the nanorod axis are observed, with PBD preferentially located at the interface with the pore wall. In comparison to the cylindrical PS-*b*-PBD system, the lamellar PS-*b*-PBD nanorods have a rounded end, rather than a depression, indicating a lower energy requirement for the curved lamellar layer. Microtome sectioning of lamellar PS-*b*-PBD nanorods perpendicular to the nanorod axis shows a morphology composed of concentric rings (Figure 5b). The outermost ring in contact with the pore wall is PBD,

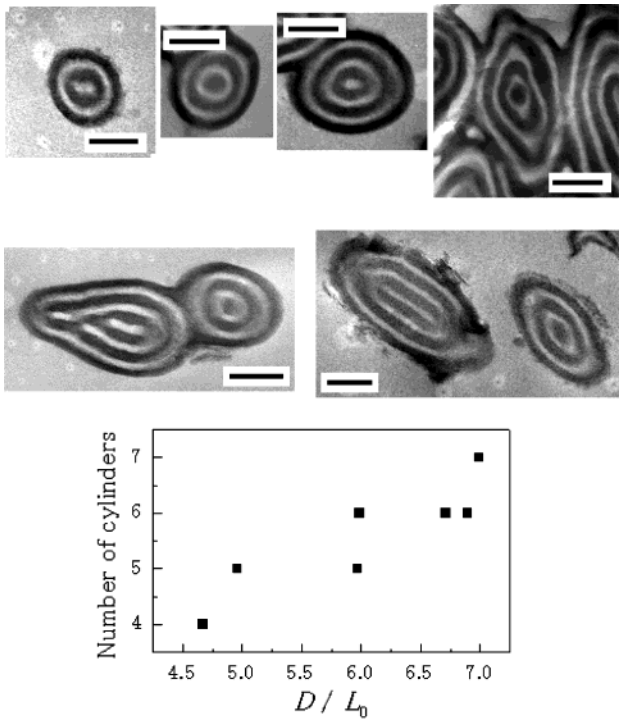

Figure 6. TEM cross-sectional images of lamellar PS-*b*-PBD in pores of different diameter. Number of cylinders vs pore diameter normalized by the equilibrium repeat spacing. Scale bars: 100 nm.

consistent with the other cross section. These results indicate that under this two-dimensional cylindrical confinement, where the diameter of the confining surfaces is large in comparison to the period and one component preferentially segregates to the walls, the symmetric PS-*b*-PBD copolymer assumes a concentric multicylinder morphology. Monte Carlo simulations and self-consistent theoretical calculations have been performed for the case of lamellar block copolymers confined within cylindrical pores. Assuming a preferential interaction between one block with the pore wall, a so-called "concentric barrel" or "dartboard" morphology was predicted.[19,20] Our results are consistent with these predictions.

Because of the variation in pore diameter for the commercial membrane, a morphology change is observed with pore diameter change (Figure 6). The outermost layer contacting the pore wall is always PBD. However, the phase at the center can either be PS or PBD, depending on the pore diameter and hence the number of PS or PBD layers. Figure 6 shows a plot of the number of cylinders as a function of the ratio of the pore diameter to the bulk, equilibrium period of the copolymer, D/L_0. As the pore diameter increases, the number of cylinders increases. However, the increase in the number of cylinders is not continuous. Rather, the number of cylinders undergoes a series of discrete increases from n to $n + 1$ cylinders where n is an integer. With an even number of cylinders PS is the central core, and with an odd number of cylinders PBD is the core. The apparent repeat period is measured by dividing the diameter of the nanorods by the number of periods. For the TEM images shown in Figure 6, all the measured repeat periods are greater than the bulk equilibrium period of 29.1 nm, and a maximum of ~44 nm is measured when the number of cylinders is four and a minimum of ~32 nm when the number of

cylinders is seven. This result indicates that the confinement of the copolymer in cylindrical pores results in a perturbation of the fundamental period of the copolymer, and the smaller the pore, the more significant is the perturbation. This, of course, must be the case since the perturbation can be distributed over more layers in the thicker nanorods and the amount of the distortion of each period can decrease. Studies are currently underway to more fully characterize the nature of this ringed structure with better defined pore geometries from membranes prepared in house.

Conclusion

In summary, self-assembly of styrene/butadiene diblock copolymers within cylindrical nanopores was investigated. Under this two-dimensional cylindrical confinement, where the pore diameter was ~200 nm, the copolymers microphase separate, yet assume morphologies that are different than those observed in the bulk. With asymmetric PS-*b*-PBD copolymers, cylindrical microdomains align along the pore axis due to the preferential wetting of the pore wall with the PBD block. Confinement effects are found to distort the natural hexagonally packing of the microdomains. In the case of lamellar PS-*b*-PBD, a concentric cylinder morphology forms within the cylindrical pores where the number of cylinders depends on the ratio of the pore diameter to the equilibrium period of the copolymer. Copolymers are drawn into the cylindrical nanoporous template by capillary force. Selective removal of the template produces nanorods of the microphase-separated copolymer. The aspect ratio of the nanorods can be made very high. Utilizing this two-dimensional confinement method, novel block copolymer morphologies were produced that have potential uses as scaffolds for isolated nanostructures.

Acknowledgment. We acknowledge the support of the National Science Foundation through the Materials Research Science and Engineering Center (DMR-0213695) and the Nanoscience Interdisciplinary Research Team (DMR-0103024) at the University of Massachusetts Amherst, the U.S. Department of Energy, Office of Basic Energy Sciences (DE-FG02-96ER45612), and Hyperstructured Organic Materials Research Center supported by the Korea Science Foundation.

References and Notes

(1) Gelb, L. D.; Gubbin, K. E.; Radhakrishnan, R.; Sliwinska-Bartkowiak, M. *Rep. Prog. Phys.* **1999**, *62*, 1573.
(2) Bates, F. S.; Frederickson, G. H. *Annu. Rev. Phys. Chem.* **1990**, *41*, 525.
(3) Turner, M. S. *Phys. Rev. Lett.* **1992**, *69*, 1788.
(4) Shull, K. R. *Macromolecules* **1992**, *25*, 2122.
(5) Kikuchi, M.; Binder, K. *Europhys. Lett.* **1993**, *21*, 427.
(6) Walton, D. G.; Kellogg, G. J.; Mayes, A. M.; Lambooy, P.; Russell, T. P. *Macromolecules* **1994**, *27*, 6225.
(7) Lambooy, P.; Russell, T. P.; Kellogg, G. J.; Mayes, A. M.; Gallagher, P. D.; Satija, S. K. *Phys. Rev. Lett.* **1994**, *72*, 2899.
(8) Brown, G.; Chakrabarti, A. *J. Chem. Phys.* **1995**, *102*, 1440.
(9) Koneripalli, N.; Singh, N.; Levicky, R.; Bates, F. S.; Gallagher, P. D.; Satija, S. K. *Macromolecules* **1995**, *28*, 2897.
(10) Kellogg, G. J.; Walton, D. G.; Mayes, A. M.; Lambooy, P.; Russell, T. P.; Gallagher, P. D.; Satija, S. K. *Phys. Rev. Lett.* **1996**, *76*, 2503.
(11) Matsen, M. W. *J. Chem. Phys.* **1997**, *106*, 7781.
(12) Pickett, G.; Balazs, A. C. *Macromol. Theory Simul.* **1998**, *7*, 249.
(13) Fasolka, M. J.; Banerjee, P.; Mayes, A. M.; Pickett, G.; Balazs, A. C. *Macromolecules* **2000**, *33*, 5702.
(14) Tang, W. H. *Macromolecules* **2000**, *33*, 1370.
(15) Radzilowski, L. H.; Carvalho, B. L.; Thomas, E. L. *J. Polym. Sci., Polym. Phys.* **1996**, *34*, 3081.
(16) Huinink, H. P.; Brokken-Zijp, J. C. M.; van Dijk, M. A.; Sevink, G. J. A. *J. Chem. Phys.* **2000**, *112*, 2452.
(17) Wang, Q.; Nealey, P. F.; de Pablo, J. J. *Macromolecules* **2001**, *34*, 3458.
(18) Knoll, A.; Horvat, A.; Lyakhova, K. S.; Krausch, G.; Sevink, G. J. A.; Zvelindovsky, A. V.; Magerle, R. *Phys. Rev. Lett.* **2002**, *89*, 035501.
(19) He, X.-H.; Song, M.; Liang, H.-J.; Pan, C.-Y. *J. Chem. Phys.* **2001**, *114*, 10510.
(20) Sevink, G. J. A.; Zvelindovsky, A. V.; Fraaije, J. G. E. M.; Huinink, H. P. *J. Chem. Phys.* **2001**, *115*, 8226.
(21) Moon, S. I.; McCarthy, T. J. *Macromolecules* **2003**, *36*, 4253.
(22) Kim, E.; Xia, Y.-N.; Whitesides, G. M. *Nature (London)* **1995**, *376*, 581.
(23) Suh, K. Y.; Kim, Y. S.; Lee, H. H. *Adv. Mater.* **2001**, *13*, 1386.

MA049299M